

# MOBILE ROBOT LOCALIZATION IN OUTDOOR ENVIRONMENTS USING COMPLEMENTARY FILTERING

**Douglas Guimarães Macharet, doug@dcc.ufmg.br**

**Armando Alves Neto, aaneto@dcc.ufmg.br**

**Víctor Costa da Silva Campos, kozttah@gmail.com**

**Mario Fernando Montenegro Campos, mario@dcc.ufmg.br**

Universidade Federal de Minas Gerais - Departamento de Ciência da Computação - Laboratório de Visão Computacional e Robótica - Belo Horizonte, MG, Brazil

**Abstract.** *As a mobile robot navigates through an indoor environment, the condition of the floor is of low (or no) relevance to its decisions, because it does not expect to find holes, rocks or other severe imperfections. In an outdoor environment, terrain characteristics play a major role on the robot's motion. Without an adequate assessment of terrain conditions and irregularities, the robot will be prone to major failures, as an external environment is typically unstructured and pavement conditions may greatly vary. Since the assumption of horizontal flat support areas is no longer valid, a mobile robot pose needs to be fully described in the three dimensional space. As such, it may assume any orientation about the three axes of its reference frame, which leads to a full six degrees of freedom configuration. The added three degrees of freedom have a major bearing on position and velocity estimation due to higher time complexity of classical techniques such as Kalman filters and particle filters. Therefore, one challenge is the identification of good models for the robotic system, which includes sensors and actuators, but that are also fast to initialize and to compute. One interesting approach that fits these requirements is the complementary filtering, which allows the summation of reliable signals in different frequency bandwidths, resulting in more accurate values in the time domain. This technique has been successfully applied to estimate the three-dimensional orientation of mobile robots, with the major advantages of having low computational cost, faster dynamic responses and simple adjustment of the parameters of the algorithm. However, the technique is basically used to calculate the angles of orientation, not taking into account signals that measure the position of the robot. This article presents a localization system for mobile robots based on the complementary filtering technique to estimate the localization and orientation, through the fusion of data from Inertial Measurement Unit (IMU), Global Positioning System (GPS) and compass. The main advantages are the low complexity of implementation and the high quality of the results for the case of navigation in outdoor environments (uneven terrain). The results obtained through this system are compared positively with those obtained using more complex and time consuming classic techniques.*

**Keywords:** *complementary filtering, localization, outdoor, mobile robots*

## 1. INTRODUCTION

Recent advances in robotics have led to the development of autonomous vehicles that navigate in outdoor environments, and much effort has been invested to increase the ability of machines to make their own decisions. However, in order to do so, some basic issues need to be addressed, such as the localization, mapping, data interpretation and fusion.

This paper presents the design, development and implementation of a localization system for mobile robots navigating in outdoor environments with uneven terrains. In the proposed methodology, we use a simple technique, called Complementary Filter (CF), to generate a good estimate of the robot's pose in the three-dimensional space.

It is fundamental that position and orientation of a mobile robot be known during the course of its navigation. While moving in an indoor environment, most of the time only the robot's pose on the plane needs to be known, and this is obtained by its position and orientation as specified by a configuration vector  $\vec{q}(t) = [ x(t) \ y(t) \ \psi(t) ]$ , in which  $x$  and  $y$  represent the position on the plane, and  $\psi$  represents the vehicle's bearing angle. The simplifying assumption in the general case is that terrain traversed by the robot is horizontal and flat. Therefore, robot navigation in indoor environments usually do not factor in ground characteristics and other anomalies on the pavement such as holes, rocks or bumps. This, however, is not the case with outdoor environments, where the terrain's topography and surface types have a major bearing on the robots displacement and navigation. For our discussion in this paper, we cluster the typical irregularities found in outdoor environments into three classes:

- Depressions and bumps;
- Slopes;
- Different types of surface (e.g. gravel, sand, asphalt, grass).

The robot will be now moving on a surface whose normal's orientation may present large variations with respect to a fixed world frame. Hence, the robot's pose needs to be specified in the three dimensional space by six degrees of freedom. The robot's pose is represented by the vector  $\vec{q}(t) = [ x(t) \ y(t) \ z(t) \ \phi(t) \ \theta(t) \ \psi(t) ]$ , in which  $z$  is the altitude,  $\theta$  and  $\phi$  are the pitch and the roll angles, respectively.

## 2. RELATED WORKS

Localization, which consists in estimating the position and orientation of mobile robot with respect to a given inertial frame, is a very hard problem, moreover for robots navigating in uneven terrains. Odometry based localization, as thoroughly described in the literature, is not viable due to several error sources such as sistematic and non-sistematic errors. Nevertheless, it is widely used for navigation on planar surfaces, which is the typical of the majority of indoor environments and the two-dimensional space. However, odometry becomes extremely limited when the position on the three-dimensional space needs to be inferred. In addition, in outdoor environments, wheel slippage is more likely to happen, which will further hinder the use of odometry.

One possible solution to address the problems inherent to odometry, is to incorporate new sensors to the system and combine all the collected data in order to improve localization. The new set of sensors may or may not provide redundant information with respect to the unknown variables. In general, one expects that the more sensors are used to measure (directly or indirectly) a given variable, the greater the confidence in the result.

One sensor that has been widely used in robotics, mainly due to the decrease in cost of Micro-Electro-Mechanical systems (MEMS) transducers, is the IMU. It is generally composed of gyros and acelerometers, orthogonally mounted on a base. In spite of all the data provided by this type of sensor, noise and bias are hard to deal with and demand careful filtering that will ultimately minimize drift and other related problems.

In [Ojeda and Borenstein, 2001], the authors use a method that makes use of fuzzy logic to estimate the attitude of a mobile robot equipped with an IMU. However, the experiments presented in the paper showed results only for two dimensional, planar displacements, which necessarily omit the inherent error produced by the system that implements odometric and inertial data provided by inertial sensors.

In most cases, inertial navigation based systems perform sensor data fusion by means of a Kalman Filter (KF). Some examples of this approach can be found in [Liu et al., 2005] and [Sukkarieh et al., 1999], where a system composed by an IMU and a GPS is shown. The fusion of data from the sensors obtained using a standard KF, which is used for linear systems. The joint use of IMU/GPS is described in [Walchko and Mason, 2002], where Extended Kalman Filter (EKF) was used, and [Li et al., 2006], where Sigma-Point Kalman Filter (SPKF) was employed for data fusion purposes. In both cases, the filters are implementations of the KF for non-linear systems. The main difficulty associated with this method is the complexity in the identification of a good model for sensors and for the robotic system. The computational complexity is also high due to intensive matrix manipulation.

A considerable number of solutions found in the literature is based on techniques for laser equipped robots that simultaneously navigate, localizing itself in the map of the environment it is concurrently building (Simultaneous localization and mapping (SLAM)). Information obtained form several sensors is combined and used to correct the estimated position and orientation during navigation.

The authors of [Müller et al., 2006] present a technique that is used by a large number of 3D SLAM works described in the literature. Usually, the robot has a laser scanner mounted facing the direction of the robot's displacement, and it is also able of rotate along the longitudinal axis. During data acquisition process, the robot moves a certain distance and stops. At that moment, the laser scanner rotates to collect the information of a specific region. These new data are aligned with the previously collected ones and this process improves the estimation of the robot's current position. The main problems faced by this method are the use of an expensive sensor (laser scanner), and the associated computational complexity.

In [Thrun et al., 2003], the SLAM technique is used for the navigation of a helicopter model, where the computational complexity problem involved in mapping and localization is one of the main issues. However, one of the drawbacks of the presented solution is that it only works if the helicopter does not pass by the same place more than once, which is not easy to guarantee as far as the robot's motion is concerned.

Alternatively to the use of Kalman Filters for the data fusion, works based on other methodologies are also found in the literature. One such methodology is the Complementary Filter, which allows the fusion of trustworthy signals with different frequency bandwidths to produce more precise signals in the time domain. This technique was used with success in aerial navigation as seen in [Iscold et al., 2007, Baerveldt and Kiang, 1997, Euston et al., 2008, Mahony and Hamel, 2007]. The main advantages of Complementary Filter are the low computational cost, the faster dynamic response and the simplicity of parameter tuning.

### 3. METHODOLOGY

The method presented in this work is divided in two parts. On the first part, the acceleration, angular velocity and magnetic orientation sensor signals are combined to generate an attitude estimate for the robot in the three-dimensional space. On the second part, this attitude is used as part of the robot's spatial position estimate, also considering the signals generated by a GPS receiver.

#### 3.1 Complementary Filter for Attitude Estimation

In this section, we present the three main stages of the first part of the methodology. They encompass the design of the Complementary Filter for attitude estimation. Initially, the output of the accelerometers are used to produce a first estimate of the roll ( $\phi$ ) and pitch ( $\theta$ ) angles of the robot. Next, an estimate of the yaw ( $\psi$ ) angle is calculated. A second estimate of these three angles is generated through the integration of the signals from the three orthogonally mounted angular velocity sensors. On the last stage, these signals are fused to generate more reliable estimates for the robot's pitch, roll and yaw angles. The results are then used to estimate the spatial localization of the robot on a later part of the methodology.

##### 3.1.1 Attitude Estimation Based on Accelerometer Measurements

The measurement of the Earth's gravity vector, by means of the three accelerometers that compose the IMU, is used to generate the first estimate of the robot's pitch and roll angles. These sensors are mounted along three orthogonal axes, as shown in Figure 1.

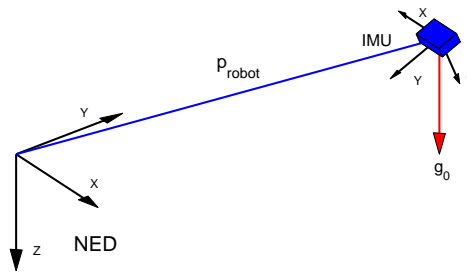


Figure 1. Gravity vector projection over the IMU axes.

To simplify the mathematics, it will be assumed that the IMU is mounted exactly on the robot's center of gravity, which is not necessarily true. However, the chosen approach works well if the difference is not very large. Therefore, we assume that the robot frame, Agent Body Coordinates (ABC), and IMU frame, are coincident. We also assume the existence of a frame fixed to the Earth's plane, usually know as North, East and Down (NED) frame. Given this arrangement, it is possible to represent the gravity acceleration vector as  $\vec{g}^{NED} = [0 \ 0 \ g_o]^T$ , which is constant in relation to the Earth's frame, and whose value is approximately  $g_o \approx 9.78 \text{ m/s}^2$ .

The gravity vector can also be described in relation to the IMU frame by multiplying  $\vec{g}^{NED}$  by a rotation matrix  $\mathbf{R}$  that relates the two axes, as seen in Equation 1. However, in order to apply this rotation, it is necessary to compute this matrix, or in other words, to know what are the sensor's orientation angles in space.

$$\vec{g}^{IMU} = {}_{NED}^{ABC} \mathbf{R}(\phi, \theta, \psi) \vec{g}^{NED}. \quad (1)$$

Stripping the above matrix equation and rewriting the angles as functions of the projection of the vector  $\vec{g}^{IMU}$  over each one of the axes from the IMU, it is possible to obtain estimates for  $\phi$  and  $\theta$  using the measurements from each of the accelerometers, as seen in equations 2 and 3.

$$\theta_a(t) = \arcsin\left(\frac{a_x(t)}{g_o}\right), \quad (2)$$

$$\phi_a(t) = \arcsin\left(\frac{a_y(t)}{-g_o \cos \theta_a(t)}\right). \quad (3)$$

Here,  $a_x(t)$  and  $a_y(t)$  represent the components of the acceleration vector measured along the IMU  $X$  and  $Y$  axes. It is important to note that a series of assumptions are made at this stage, by considering the estimated values. First, besides being displaced on the robot's center of gravity, the sensors were mounted along perfectly orthogonal axes. Therefore, the measurements to not present misalignment bias, or if it exists, it is negligible. In addition, there are no other biases on the sensors, and the measurement noise is additive, approximately normal with zero mean.

Another important point is that Equation 2 may present singularity problems for  $\theta_a = \pm\pi/2$  angles. However, under normal operating conditions, the robot's pitch angle is restricted to values smaller  $\pi/2$ . Likewise, it is assumed that the roll angle is restricted to even lower bounds than those of the pitch, making it unnecessary to use the  $a_z$  information.

An important assumption is that, at each time instant, the accelerometer is measuring only the gravity vector. This assumption is only valid when the robot is an inertial state. Although restrictive, this assumption is valid for the range of movements performed by ground mobile robots. Therefore, the low frequency signals from the accelerometers provide reliability to the estimate of  $\phi$  and  $\theta$ . It will be shown later that this information will be combined with the information from the gyros and magnetometers mounted on the robot.

### 3.1.2 Attitude Estimation Based on Magnetometers Measures

As it was previously seen, it is not possible to estimate the robot's orientation relative to the Earth's North by using acceleration sensors alone, and therefore a sensor that is capable of providing the robot's orientation with respect to the Earth's plane is required. A digital compass, composed of two orthogonally mounted magnetometers, mounted on a plane parallel to the Earth's plane, was used in our experiments.

The  $\psi_m(t)$  represents a previous estimate of the robot's heading relative to the NED frame, complementing the angular information from the previous section. Equation 4 computes the robot's yaw angle as a function of the magnetometers measurements  $m_x(t)$  and  $m_y(t)$  in the compass frame.

$$\psi_m(t) = \arctan \left[ \frac{m_y(t)}{m_x(t)} \right]. \quad (4)$$

### 3.1.3 Attitude Estimation Based on Gyrometers Measurements

Besides the accelerometers, the IMU contains three gyroscopes (gyros) that measure the robot's angular velocities about the ABC frame axes. A second estimate for  $\phi(t)$ ,  $\theta(t)$  and  $\psi(t)$  can be obtained by integrating the differential kinematic equations that describe the system.

As previously seen, the problem is that the mathematics of the attitude parameters using Euler angles representation present singularities in some of its configurations. This can be harmful to the signal integration process, since it generates rough variations on the final results. Therefore, we chose to use quaternions to represent rotations.

The vehicle's spatial orientation is then by  $\vec{Q}(t) = [q_0(t) \ q_1(t) \ q_2(t) \ q_3(t)]$ , and the pitch, roll and yaw angles are estimated by Equations 5, 6 and 7, respectively.

$$\theta_g(t) = -\arcsin [-2(q_1(t)q_3(t) + q_0(t)q_2(t))], \quad (5)$$

$$\phi_g(t) = -\arctan \left[ \frac{2(q_2(t)q_3(t) + q_0(t)q_1(t))}{q_0(t)^2 - q_1(t)^2 - q_2(t)^2 + q_3(t)^2} \right], \quad (6)$$

$$\psi_g(t) = -\arctan \left[ \frac{2(q_1(t)q_2(t) + q_0(t)q_3(t))}{q_0(t)^2 + q_1(t)^2 - q_2(t)^2 - q_3(t)^2} \right]. \quad (7)$$

The quaternion values, in turn, are obtained by integrating Equation 8, where  $g_x(t)$ ,  $g_y(t)$  and  $g_z(t)$  are the angular velocities corresponding to the roll, pitch and yaw angles, respectively:

$$\dot{\vec{Q}}(t) = \frac{1}{2} \begin{pmatrix} 0 & -g_x(t) & -g_y(t) & -g_z(t) \\ g_x(t) & 0 & g_z(t) & -g_y(t) \\ g_y(t) & -g_z(t) & 0 & g_x(t) \\ g_z(t) & g_y(t) & -g_x(t) & 0 \end{pmatrix} \vec{Q}(t). \quad (8)$$

The initial step of the integration process is determined by the initial attitude estimate obtained by the projection of the gravity vector and the North's heading at time zero, as expressed by Equation 9.

$$\vec{Q}(0) = - \begin{pmatrix} \cos \frac{\phi_a(0)}{2} \cos \frac{\theta_a(0)}{2} \cos \frac{\psi_m(0)}{2} + \sin \frac{\phi_a(0)}{2} \sin \frac{\theta_a(0)}{2} \sin \frac{\psi_m(0)}{2} \\ \sin \frac{\phi_a(0)}{2} \cos \frac{\theta_a(0)}{2} \cos \frac{\psi_m(0)}{2} + \cos \frac{\phi_a(0)}{2} \sin \frac{\theta_a(0)}{2} \sin \frac{\psi_m(0)}{2} \\ \cos \frac{\phi_a(0)}{2} \sin \frac{\theta_a(0)}{2} \cos \frac{\psi_m(0)}{2} + \sin \frac{\phi_a(0)}{2} \cos \frac{\theta_a(0)}{2} \sin \frac{\psi_m(0)}{2} \\ \cos \frac{\phi_a(0)}{2} \cos \frac{\theta_a(0)}{2} \sin \frac{\psi_m(0)}{2} + \sin \frac{\phi_a(0)}{2} \sin \frac{\theta_a(0)}{2} \cos \frac{\psi_m(0)}{2} \end{pmatrix}. \quad (9)$$

In this case, the IMU does not need to be close to the vehicle's center of gravity. However the bias of the MEMS gyros can distort the velocity measurements, producing destructive effects on the numerical integration process. The drift caused by this effect produces a low frequency error that hinders the direct use of this process.

On the following development, it is assumed that there is no sensor bias and that noise is gaussian with zero mean. Then, it is shown that these assumptions are valid, and how the accelerometers, magnetometers and gyroscopes data may be combined by a complementary filtering process.

### 3.1.4 Attitude Data Fusion

The output of execution of the previous stages is a pair of estimates from the IMU and the compass of the robot's attitude. As already discussed, the values of  $\phi_a(t)$ ,  $\theta_a(t)$  and  $\psi_m(t)$  are reliable as long as the vehicle performs slow movements, in other words, as long as it moves in an approximately inertial way. On the other hand, the parameters  $\phi_g(t)$ ,  $\theta_g(t)$  and  $\psi_g(t)$  are susceptible to errors due to the integration of low frequency noise, being, therefore, reliable under larger variations.

Based on these assumptions, a data fusion that considers only the most reliable frequency range of each signal, so as to generate the most reliable result, should be performed. Complementary Filtering is a natural choice, since it is composed of two digital filters, a lowpass and a highpass, with the same cut-off frequency  $\omega_c$ . For the experiments presented in the next section of this work, first order digital filters with maximally plane response on the passband (Butterworth) and 10 Hz sampling rate were used. A typical frequency response of the CF filter can be seen on Figure 2.

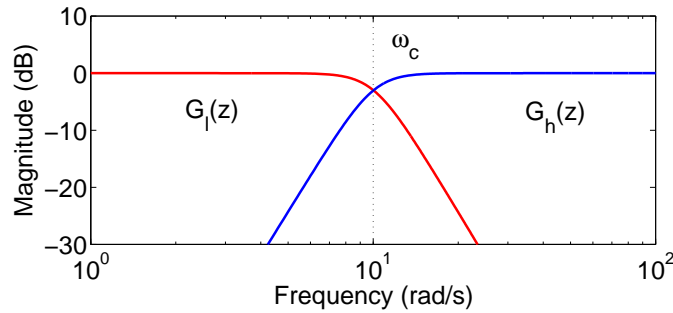


Figure 2. Frequency response of complementary filters with cut-off frequency  $\omega_c$ .

The first filter significantly attenuates the high frequency accelerations of the first estimate (gravity projection) and the noise from the magnetometers data. The second filter suppresses the low frequency errors of the second estimate (gyros integration). The filtering process is performed by a convolution in the time domain, as can be seen in Equations 10, 11 and 12. Finally, the two signals are summed in time, generating the final estimate of the pitch, roll and yaw angles.

$$\phi(t) = G_l(t) * \phi_a(t) + G_h(t) * \phi_g(t), \quad (10)$$

$$\theta(t) = G_l(t) * \theta_a(t) + G_h(t) * \theta_g(t), \quad (11)$$

$$\psi(t) = G_l(t) * \psi_m(t) + G_h(t) * \psi_g(t). \quad (12)$$

## 3.2 Complementary Filter for Position Estimation

In this section, we describe the second part of the methodology. A second Complementary Filter is designed to combine the position estimates given by the robot's odometry sensors and by the GPS sensor, producing a more reliable and more accurate final estimate of the robot's localization on the six dimensional configuration space.

### 3.2.1 Position Estimation Based on GPS Measures

On the first stage of this second part, a Global Positioning System signal receiver fixed to the robot's body was used to obtain an estimate of its global positioning. Usually, this estimate is given as a function of the latitude, longitude and altitude of the receiver with respect to the Earth's surface.

In this work, however, it is not necessary to know the robot's position relative to the terrestrial inertial reference, since the displacements will be very small compared to the Earth's radius. Hence, it is possible to assume that the Earth is approximately planar throughout the robot's navigation space. A coordinate transformation from latitude, longitude and altitude of the GPS to the differential manifold of the Euclidian tridimensional space coincident with the NED frame is performed, and the GPS out put may be considered as the  $x_g(t)$ ,  $y_g(t)$  and  $z_g(t)$  signals.

An interesting feature of using the CF technique is that the GPS signal, just as it happens with all sensors, contains noise and other variations. In the specific GPS case, one such effect which potentially has a large impact on localization is known as *random walk*. Random walk is caused by high frequency variations which corrupt the satellite signals when the receiver is either stopped or moving slowly. This, and other similar undesirable effects, can be discarded by filtering out the signal with a low pass filter.

### 3.2.2 Position Estimation Based on Attitude and Odometry

Once the robot's attitude in the tridimensional space is known, the next step consists of estimating the robot's position. One simple solution is to integrate the kinematic differential equation (Equation 13) which describes the robot's movement

in space.

$$\begin{bmatrix} \dot{x}_o(t) \\ \dot{y}_o(t) \\ \dot{z}_o(t) \end{bmatrix} = v_o(t) \begin{bmatrix} \cos \psi(t) \cos \theta(t) \\ \sin \psi(t) \cos \theta(t) \\ \sin \theta(t) \end{bmatrix}, \quad (13)$$

where  $v_o(t)$  is the measured velocity given by the robot's odometry sensor over time, and  $\psi(t)$  and  $\theta(t)$  are the angles estimated on the first part of our methodology. The integration of this equation generates the  $x_o(t)$ ,  $y_o(t)$  and  $z_o(t)$  signals relative to the robot's odometry.

Just as in the previous part, the estimation of a signal by numerical integration generates a measurement that is not reliable due to bias and other sensor noises from sensors. The integration process tends to amplify the lower frequency signals of the variable, creating a drift over time. Thus, in a complementary way to the GPS signal, the position estimations by odometry may be considered as more reliable at higher frequencies. The two data streams are then combined using a second Complementary Filter.

### 3.2.3 Position Data Fusion

Just as in the first part of the methodology, two different estimates were generated for each one of the variables that we wish to obtain. These information present reliable information over different frequency ranges and the fusion of these data should be factored in.

For that reason, the complementary filtering technique was used, in which two filters  $G_l$  and  $G_h$  with cut-off frequency  $\omega_c$  (whose value is not necessarily the same as the previous one). Equations 14, 15 and 16 show the calculation of the final values for the robot's position.

$$x(t) = G_l(t) * x_g(t) + G_h(t) * x_o(t), \quad (14)$$

$$y(t) = G_l(t) * y_g(t) + G_h(t) * y_o(t), \quad (15)$$

$$z(t) = G_l(t) * z_g(t) + G_h(t) * z_o(t). \quad (16)$$

Finally, the vector that represents the robot's behavior over time on the configuration space is given: 17.

$$\vec{q}(t) = [ x(t) \quad y(t) \quad z(t) \quad \phi(t) \quad \theta(t) \quad \psi(t) ]. \quad (17)$$

### 3.3 Computational Complexity Analysis

Gaussian Filters, such as Kalman Filter and its derivations (KF, EKF, UKF), are very commonly used in data fusion. The most expensive steps of Kalman Filters are the matrix operations (multiplication, inversion). The asymptotically fastest algorithm known for matrix multiplication is the Coppersmith-Winograd algorithm [Coppersmith and Winograd, 1987], with complexity of  $O(d^{2.376})$ , where  $d$  represents the size of the square matrix. In the specific case of Kalman Filters, this size is defined by the number of state variables estimated [Thrun et al., 2005]. Here we consider six variables (three positions and three angles).

It is known that the computational cost of the Particle Filter technique depends on the number of particles  $m$  that we desire to use. The larger the number of particles, the greater the accuracy of the localization of the robot. According to [Thrun et al., 2005], the computational complexity of this method is given by  $O(m \log m)$ . The main problem with this is that the number of particles grows exponentially with the number of states  $d$ , which in practice is intractable for three-dimensional space.

The Complementary Filter technique is based on digital filtering theory. The Butterworth filter algorithm has a complexity that is proportional to the order  $n$  of the filter, or in other words, it is given by  $O(n)$ . The proposed methodology uses a filter to estimate each of the variables of the state vector ( $\vec{q}$ ). It leads to a complexity of  $O(nd)$ , where  $d$  represents the number of variables of the state vector. Therefore, our methodology has a linear complexity, which is less than half of the complexity of frequently used techniques such as Unscented Kalman Filter (UKF).

## 4. EXPERIMENTS

The experiments were performed offline using real data acquired by a mobile robot while traversing an outdoor environment. During the robot's navigation process, it collected and saved all sensor data, which were used as input to the simulation program.

The robot used was a Pioneer P3-AT model dedicated to external applications. It has a good load capacity, and data collection is performed by a laptop on it, also responsible for sending commands to the robot. Figure 3 shows the arrangement of sensors on the robot.

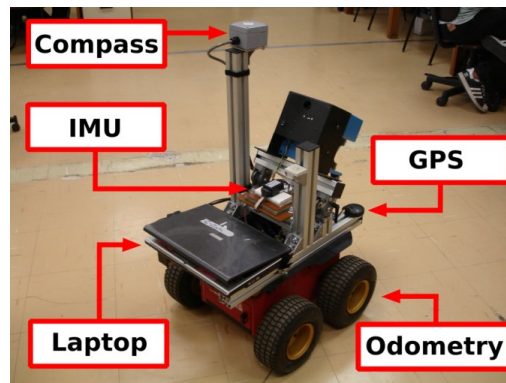


Figure 3. Equipments used in the real experiments.

In order to compute the attitude and position of the robot, the information provided by an IMU, a GPS, a digital compass, and the robot's odometry sensor were used. The IMU was the *Crista* by *Cloud Cap Technologies* and composed of three mutually orthogonal gyroscopes and three orthogonal accelerometers. A Garmin 18x-5Hz GPS was also used. It provides the absolute values of geographic position of the robot around the world. This information was used in terms of the Easting and Northing coordinates (from the coordinate system Universal Transverse Mercator, also called UTM), that are given in meters. Our set of sensors is completed by a KVH C-100 Digital Compass, that is responsible for providing absolute values for the orientation of the robot according to the Earth's magnetic north. It is composed by two magnetometers disposed orthogonally in a planar form, and their values can be read directly from a serial interface.

In order to simplify the calculations it is assumed that the IMU is mounted exactly at the robot's center of gravity, which in practice may not be exactly true. Since the difference is very small and the speed of the robot is small, the setup is suitable for our approach. Hence, it is assumed that the robot and the IMU reference frame are coincident. Two experiments were planned and carried out using the aforementioned setup, and they are describe next.

#### 4.1 EXPERIMENT 1

In this first experiment the robot performed a path composed, mainly, of straight lines and well defined curves (approximately  $90^\circ$ ). The main objectives were to verify the accuracy of the robot's localization, and to verify the possibility of correcting odometric errors by incorporating GPS data.

Figure 4(a) shows a comparison between three paths: the first one was performed by the robot based on the raw GPS data; the second, computed using our methodology, and the third path estimated by an UKF [Julier and Uhlmann, 1997, Thrun et al., 2005]. As show in the figure, the raw GPS data is very noisy and clearly provides very low accuracy if used directly. The values obtained using our methodology, however, provided a smoother path closer to the one actually executed by the robot. It is interesting note that the result was very similar to the one obtained by more complex techniques such as UKF.

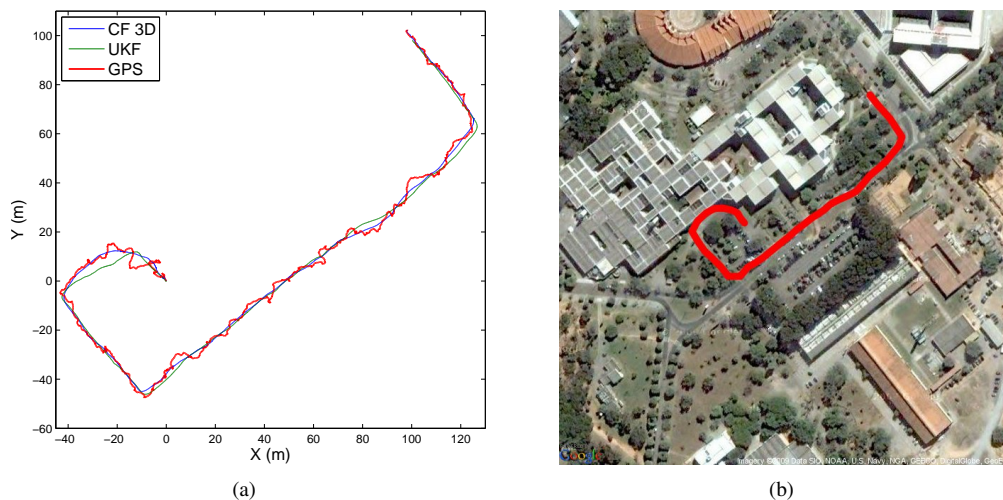


Figure 4. Reconstruction of the path done by the robot on Experiment 1.

The use of the GPS made it possible to correct the velocity errors in odometric measurements. Another benefit of using GPS data is the possibility to obtain the robot's global localization. In order to verify how close the robot's self localization

from the actual executed path, both paths were drawn on a satellite image using an API [Google Maps API, 2008]. Figure 4(b) shows the path executed by the robot over an image of the region where the experiments were performed.

As observed in Figure 5, the data still contains a small amount of noise, however, the results were adequate for our purposes, and it represents the actual displacement performed by the robot. Analyzing the standard deviation of the data we have  $\sigma_\phi = 2.4^\circ$ ,  $\sigma_\theta = 2.2^\circ$ , while using the UKF the standard deviations are  $\sigma_\phi = 1.8^\circ$ ,  $\sigma_\theta = 1.9^\circ$ . We chose to not calculate  $\sigma_\psi$ , since the mean is not a good representation of the values obtained.

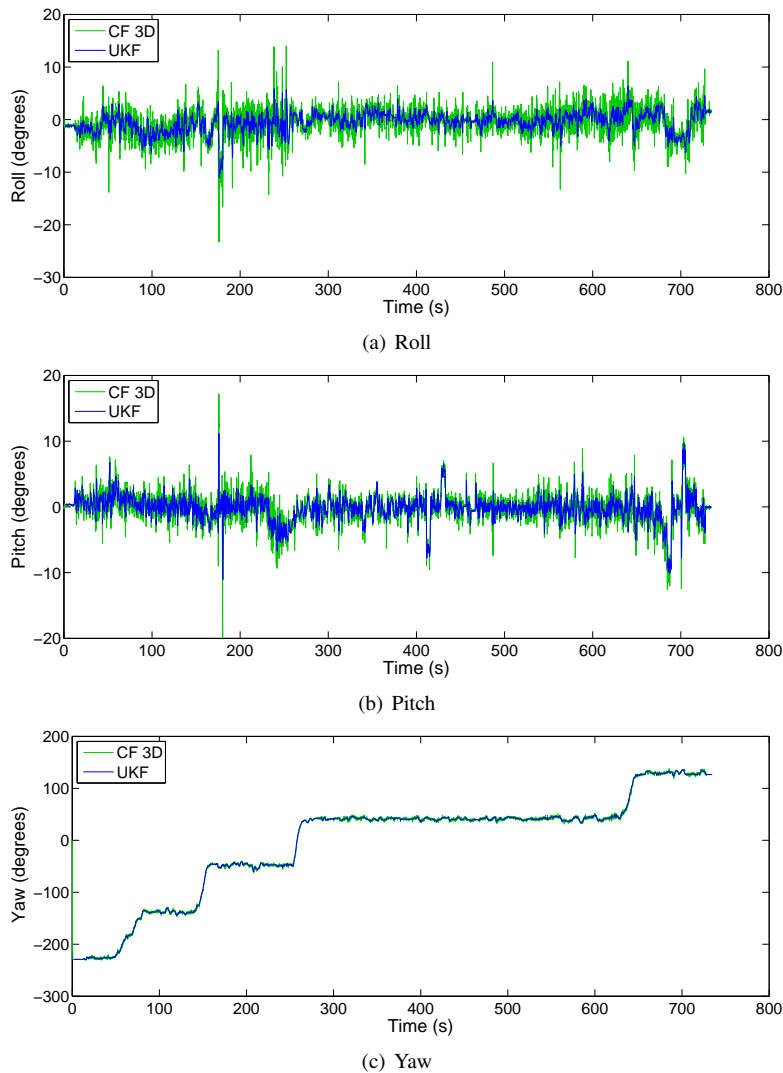


Figure 5. Calculated orientation angles on Experiment 1.

The angle  $\phi$  (Figure 5(a)) showed small variations due to imperfections in the terrain and signal noise, but at the end of the experiment it is possible to observe a larger variations ( $\approx -4^\circ$ ) when the robot starts to descend a ramp.

The values of  $\theta$  have, for the most part, zero mean (flat terrain), however, between  $t = 230s$  e  $t = 270s$  (Figure 5(b)) the variation ( $\approx -2^\circ$ ) occurred while it descended an inclined region of the terrain where the experiment was carried out. Three other relevant disturbances, also related to terrain inclination, can be seen in the graph.

The result of  $\psi$  can be verified directly, since during the path the robot took four sharp turns ( $90^\circ$  curves) that can be clearly seen in Figure 5(c), represented by four large steps.

## 4.2 EXPERIMENT 2

Another experiment was performed, and the robot's trajectory was composed by a path with different kinds of ramps. The main objective was to verify the estimation of the variation on the Z axis. The images on Figure 6 show the estimated trajectory for the navigation performed by the robot during the experiment.

The values of altitude returned from the GPS are fundamental for the computation of the variation in the Z axis. Unfortunately, this value shows a large variation, and as such it is not a good representation of the actual displacement of the robot.



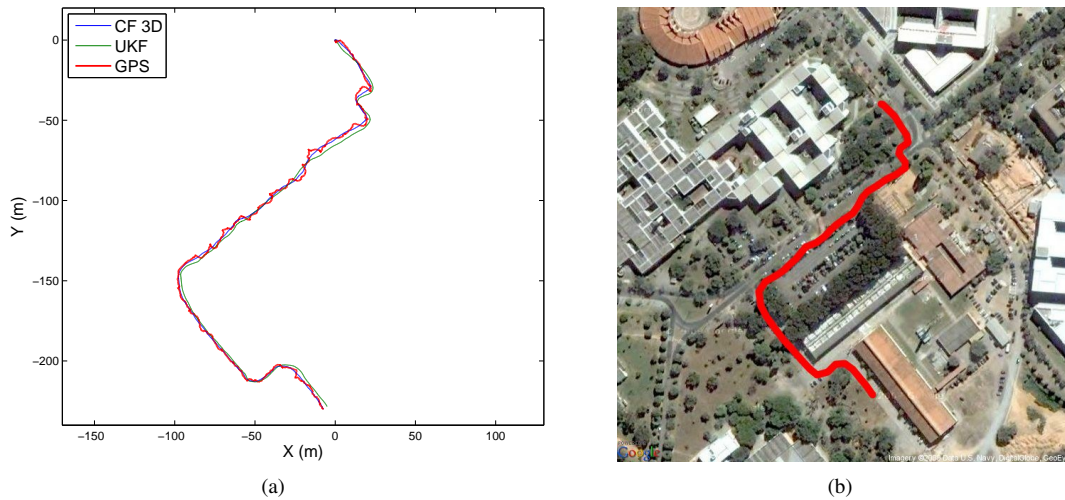


Figure 6. Reconstruction of the path performed by the robot in Experiment 2.

Figure 7 shows a comparison among the altitude calculated by our methodology, the altitude computed by integrating the kinematic equation  $z_o(t)$  (Equation 13), and the altitude  $z_g(t)$  obtained directly from the GPS. Small variations on the Z axis can be clearly observed at time instants  $t \approx 25s$ ,  $t \approx 130s$ ,  $t \approx 290s$  and  $t \approx 460s$ . The difference between the values of the highest and the lowest points returned from the GPS is  $\approx 12m$ , a value which is not consistent with the actual movement performed by the robot, which is well represented by the information obtained from  $z_o(t)$ .

Thus, the computed values for the variation in altitude were not reliable, and further analysis should be performed for an adequate incorporation of altitude data provided by the GPS. For the moment, and with the technology that was available to us, the measurements provided by the GPS contains much uncertainty. As a matter of fact, a more precise altitude data is required in order to correct the Z using our methodology as well as others, such as UKF.

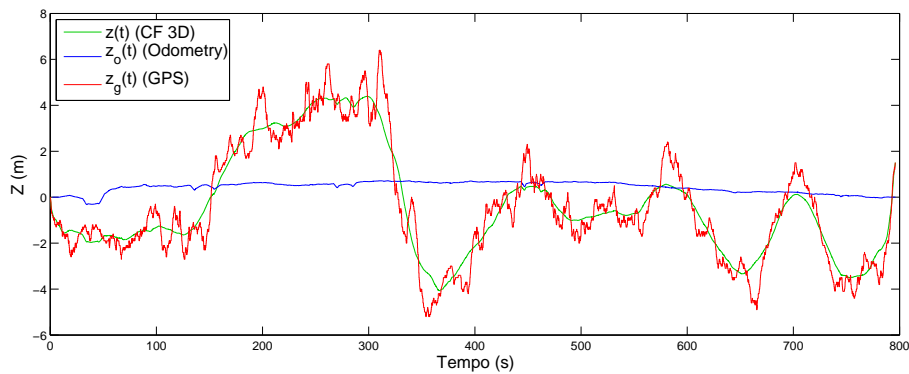


Figure 7. Altitude comparison for the complementary filtering using GPS.

## 5. CONCLUSIONS AND FUTURE WORKS

This work presented the use of the Complementary Filter technique to estimate the full pose (localization and orientation) in the configuration space, for mobile robots navigating in outdoor environments on uneven terrain. The main advantage of the proposed technique is the significant reduction of the computational complexity of the overall system, which enables increasing the sampling frequency of the signals with a consequent improvement in the accuracy of the estimates.

The results were satisfactory and very close to the values obtained with more complex techniques such as the Unscented Kalman Filter. This has been shown by plotting the actual path on satellite images, where the estimated path performed by using the proposed methodology have shown to be faithful to the actual path performed by the robot. We have also shown that height (change in Z axis) estimation was less accurate, mainly due to the large uncertainty on the altitude data provided by the GPS.

It was possible to obtain a good estimation of the orientation angles  $(\phi, \theta, \psi)$ , but they still have a certain amount of noise. The most accurate and reliable value was  $\psi$ , mainly due to the use of a digital compass, which made it possible to eliminate drift.

Although the experiments were conducted in an offline way (post navigation processing), it was possible to observe

that the method is very efficient, and amenable to be used in real time.

As future work, further experiments will be performed with larger vehicles, since it will make it possible to analyze the behavior of the system on greater scale experiments where the vehicle's size is comparable to the path width restrictions.

Sensor processing continues to be an area of great relevance for robotics. Further investigation is demanded on sensors imperfections, such as bias in the IMU accelerometers and gyros, in order to provide better methods to minimize even further their effects on the final estimations. Likewise, issues arising in other sensors such as magnetometers must be dealt with adequately. We also plan to research on novel techniques to make the methodology robust to GPS problems, like signal loss and random walk. One possibility is to adjust the cut-off frequency or making its value adaptive.

Finally, the estimation of the variation in the altitude of the robot is very problematic, and it can be the source of a large amount of errors in the system. To tackle this problem, it is necessary to perform better analysis and treatment of the GPS altitude data. Other sensors, such as accurate differential pressures sensors, may be considered as an alternative to GPS altitude data.

## 6. ACKNOWLEDGEMENTS

The authors would like to thank Wolmar Pimenta for the support on the construction and integration of the mechanical system used in the experiments, and the financial support offered by the Fundação de Amparo a Pesquisa do Estado de Minas Gerais (FAPEMIG), the Conselho Nacional de Desenvolvimento Científico e Tecnológico (CNPq), and the Coordenação de Aperfeiçoamento de Pessoal de Nível Superior (CAPES).

## 7. REFERENCES

- Baerveldt, A.-J. and Klang, R. (1997). A Low-cost and Low-weight Attitude Estimation System for a Autonomous Helicopter. In *IEEE International Conference*.
- Coppersmith, D. and Winograd, S. (1987). Matrix multiplication via arithmetic progressions. In *STOC '87: Proceedings of the nineteenth annual ACM symposium on Theory of computing*, pages 1–6, New York, NY, USA. ACM.
- Euston, M., Coote, P., Mahony, R., Kim, J., and Hamel, T. (2008). A complementary filter for attitude estimation of a fixed-wing uav. In *Proceedings of IEEE/RSJ International Conference on Intelligent Robots and Systems (IROS)*, pages 340–345.
- Google Maps API (2008). Google Maps API - Google Code. Available at: <http://code.google.com/apis/maps/>. Accessed on: July 29, 2008.
- Iscold, P., de Oliveira, G. R. C., Neto, A. A., Pereira, G. A. S., and Torres, L. A. B. (2007). Desenvolvimento de Horizonte Artificial para Aviação Geral baseado em Sensores MEMS. In *V Congresso Brasileiro de Engenharia Inercial*, Rio de Janeiro.
- Julier, S. and Uhlmann, J. K. (1997). A new extension of the kalman filter to nonlinear systems. In *Proceedings of The 11th Int. Symp. on Aerospace/Defense Sensing, Simulation and Controls, Multi Sensor Fusion, Tracking and Resource Management*.
- Li, Y., Wang, J., Rizos, C., Mumford, P., and Ding, W. (2006). Low-cost Tightly Coupled GPS/INS Integration Based on a Nonlinear Kalman Filtering Design. In *National Technical Meeting of the Institute of Navigation*, pages 958–966.
- Liu, B., Adams, M., and Ibañez-Guzmán, J. (2005). Multi-aided Inertial Navigation for Ground Vehicles in Outdoor Un-even Environments. In *Proceedings of IEEE International Conference on Robotics and Automation (ICRA)*, Barcelona, Espanha.
- Mahony, R. and Hamel, T. (2007). *Advances in Unmanned Aerial Vehicles: State of the Art and the Road to Autonomy*, chapter Robust Nonlinear Observers for Attitude Estimation of Mini UAVs, pages 343–376. Springer.
- Müller, M., Surmann, H., Pervözl, K., and May, S. (2006). The Accuracy of 6D SLAM using the AIS 3D Laser Scanner. In *IEEE International Conference on Multisensor Fusion and Integration for Intelligent Systems*, Heidelberg, Germany.
- Ojeda, L. and Borenstein, J. (2001). Improved Position Estimation for Mobile Robots on Rough Terrain Using Attitude Information. Technical report, The University of Michigan.
- Sukkarieh, S., Nebot, E. M., and Durrant-Whyte, H. F. (1999). A high integrity IMU/GPS navigation loop for autonomous land vehicle applications. In *Proceedings of IEEE Transactions on Robotics and Automation*, pages 572–578.
- Thrun, S., Burgard, W., and Fox, D. (2005). *Probabilistic Robotics*. The MIT Press.
- Thrun, S., Diel, M., and Hähnel, D. (2003). Scan Alignment and 3D Surface Modeling with a Helicopter Platform. In *Proceedings of the International Conference on Field and Service Robotics*, Lake Yamanaka, Japan.
- Walchko, K. J. and Mason, P. A. C. (2002). Inertial Navigation. In *Florida Conference on Recent Advances in Robotics*.

## 8. Responsibility notice

The authors are the only responsible for the printed material included in this paper.